In vivo 7 Tesla imaging of the dentate granule cell layer in Schizophrenia

Ivan I. Kirov, PhD[a], **Caitlin J. Hardy, MD**[a,b], **Kant Matsuda, MD, PhD**[c], **Julie Messinger, PhD**[b], **Ceylan Z. Cankurtaran, MD**[a], **Melina Warren, MD**[a], **Graham C. Wiggins, PhD**[a], **Nissa N. Perry, MA**[a], **James S. Babb, PhD**[a], **Raymond R. Goetz, PhD**[b,d], **Ajax George, MD**[a], **Dolores Malaspina, MD**[b], and **Oded Gonen, PhD**[a]

[a]Department of Radiology, 660 First Avenue, New York, NY 10016, USA

[b]Department of Psychiatry, 550 First Avenue New York, NY 10016, USA

[c]Department of Pathology, 550 First Avenue, New York, NY 10016, USA

[d]New York State Psychiatric Institute, Div. Clinical Phenomenology, 1051 Riverside Dr., Unit 123, New York, NY 10032, USANew York University School of Medicine

Abstract

PURPOSE—The hippocampus is central to the pathophysiology of schizophrenia. Histology shows abnormalities in the dentate granule cell layer (DGCL), but its small size (~100 micron thickness) has precluded in vivo human studies. We used ultra high field magnetic resonance imaging (MRI) to compare DGCL morphology of schizophrenic patients to matched controls'.

METHOD—Bilateral hippocampi of 16 schizophrenia patients (10 male) 40.7±10.6 years old (mean ±standard deviation) were imaged at 7 Tesla MRI with heavily T_2^*-weighted gradient-echo sequence at 232 micron in-plane resolution (0.08 μL image voxels). Fifteen matched controls (8 male, 35.6±9.4 years old) and one ex vivo post mortem hippocampus (that also underwent histopathology) were scanned with same protocol. Three blinded neuroradiologists rated each DGCL on a qualitative scale of 1 to 6 (from "not discernible" to "easily visible, appearing dark gray or black") and mean left and right DGCL scores were compared using a non-parametric Mann-Whitney test.

RESULTS—MRI identification of the DGCL was validated with histopathology. Mean right and left DGCL ratings in patients (3.2±1.0 and 3.5±1.2) were not statistically different from controls' (3.9±1.1 and 3.8±0.8), but patients' had a trend for lower right DGCL score (p=0.07), which was

Corresponding Author: Oded Gonen PhD, Department of Radiology, New York University School of Medicine, 660 First Avenue, 4th Floor, New York, New York 10016, Telephone/FAX: (212) 263-3532/(212) 263-7541, oded.gonen@nyumc.org.

CONFLICT OF INTEREST
None of the authors report competing interest

CONTRIBUTORS
OG and DM designed the study. GCW wrote the imaging protocol. IIK and CJH managed the literature searches. CJH performed the data processing. JSB and RRG undertook the statistical analysis. KM carried out the histopathology. CZC, MW and AG were the radiologists who scored the images. CJH wrote the first draft of the manuscript. IIK wrote the final draft of the manuscript. JM and NP evaluated and consented the patients. All authors contributed to and have approved the final manuscript.

Publisher's Disclaimer: This is a PDF file of an unedited manuscript that has been accepted for publication. As a service to our customers we are providing this early version of the manuscript. The manuscript will undergo copyediting, typesetting, and review of the resulting proof before it is published in its final citable form. Please note that during the production process errors may be discovered which could affect the content, and all legal disclaimers that apply to the journal pertain.

significantly associated with patient diagnosis (p=0.05). The optimal 48% sensitivity and 80% specificity for schizophrenia was achieved with a DGCL rating of   2.

CONCLUSION—Decreased contrast in the right DGCL in schizophrenia was predictive of schizophrenia diagnosis. Better utility of this metric as a schizophrenia biomarker may be achieved in future studies of patients with homogeneous disease subtypes and progression rates.

Keywords

dentate granule cell layer; ultra high field MRI; structural MRI; imaging

1. INTRODUCTION

Although psychotic symptoms are well recognized in schizophrenia, cognitive deficits are the other key feature. They precede the emergence of psychosis and are strongly related to functional outcome, including decrements in verbal learning and memory, reasoning and problem solving (Larson et al., 2010). Given the early, 16–30, age of onset (Mueser and Penn, 2004), and its life long consequences, it is imperative to advance our understanding of the underlying biology of both types of symptoms in order to facilitate new treatment paradigms and to develop the (non invasive) markers to monitor them.

Abnormalities in the hippocampus have been described as central to the pathophysiology of schizophrenia (Harrison, 2004) and have been hypothesized to give rise not only to the cognitive, but also to the positive symptoms of the disease (Bast, 2011; Small et al., 2011). Much of the support for these arguments comes from in vivo imaging studies showing decreased volume and abnormal activation, cerebral blood flow (Tamminga et al., 2010), as well as connectivity (Benetti et al., 2009) in the hippocampus of patients. Most of these studies, however, could not investigate the involvement of specific hippocampal subfields, because their cytoarchitectural boundaries are not clearly identifiable in magnetic resonance imaging (MRI) data acquired at 1.5 and 3 Tesla magnet strength. Computation-heavy approaches developed to circumvent this limitation have found lower volumes (Narr et al., 2004) and hypermetabolism (Schobel et al., 2009b) in the cornu ammonis (CA).

Beyond these handful of studies, however, hippocampal subfield pathology in schizophrenia has only been shown in animal models and post-mortem in humans (Tamminga et al., 2010). In addition to the CA region, these also implicate the dentate gyrus, and in particular, its dentate granule cell layer (DGCL), the ~100 micron thick site of neuron proliferation and maturation (Ming and Song, 2011). In schizophrenia, the DGCL shows abnormal morphology (Lauer et al., 2003), and decreased neurogenesis (Reif et al., 2006). Multiple genes associated with neuronal development (Altar et al., 2005; Rioux and Arnold, 2005), including schizophrenia susceptibility genes, e.g. neuregulin-1, disrupted-in–schizophrenia 1 (DISC1) and dysbindin (Harrison and Weinberger, 2005), are expressed in the DGCL (Law et al., 2004; Meyer and Morris, 2009; Weickert et al., 2008).

This evidence, and a recent study demonstrating that the DGCL can be consistently visualized in vivo with ultra high filed, 7 Tesla, MRI (Prudent et al., 2010), motivated us to test the hypothesis that DGCL morphology is abnormal in schizophrenia, and to assess the sensitivity and specificity of the (clinically feasible) imaging approach.

2. METHODS

2.1 Human Subjects

Twenty five (14 male, 11 female, 40.2±10.4 years old) patients with confirmed schizophrenia were prospectively recruited from an outpatient clinic. Sixteen age and gender

matched controls (8 male, 8 female, 36.1 ± 9.2 years old) were recruited from medical center and Internet postings. All subjects were assessed with the Diagnostic Interview for Genetic studies (DIGS) (Nurnberger et al., 1994) which establishes diagnoses of 31 major mood and psychiatric disorders (covering DSM-III-R criteria of common Axis I and Axis II disorders). DIGS was administered by Masters level or above interviewers trained to gold standards of reliability. Inclusion criteria were 18 – 55 years old and capacity to consent, and for the patients, diagnosis of schizophrenia. Exclusion criteria were as follows. All subjects: substance abuse in the past 6 months, MRI contraindication or inability to tolerate the MRI exam. Patients: uncontrolled medical illness, other psychiatric or neurological disorders. Controls: current psychiatric disorders, Axis I disorders in the past two years, personal or family history of psychosis, neurological disorders and history of traumatic brain injury. Current symptoms were assessed using the Positive and Negative Syndrome Scale (PANSS) (Kay et al., 1987; Kay et al., 1992; Kay et al., 1989). Both the original PANSS scales (positive, negative and general psychopathology scale) and the newer pentagonal PANSS symptom factors (positive, negative, activation, dysthymia and autistic preoccupation) (White et al., 1997) were examined. In addition, an intact ex vivo hippocampus from a 68 year old woman who died from pneumonia was obtained from autopsy material in order to compare its MRI with histopathology that is otherwise unlikely to be available from the relatively young schizophrenia patients and their controls. This study was approved by the Institutional Review Board of New York University School of Medicine and written informed consent was obtained from all subjects.

2.2 MRI

MRI was done in a 7 Tesla whole-body scanner (Magnetom, Siemens AG, Erlangen, Germany) using a volume-transmit 24-coil head receive-array (Nova Medical, Boston, MA). After placing each subject head-first supine into the magnet, localizer images were obtained in three planes to verify head placement. This was followed by 5 minutes of 3D T_1-weighted sagittal Magnetization-Prepared-Rapid-Acquisition-Gradient-Echo (MP-RAGE) MRI: TE/ TR/TI: 2.6/2600/ 1100 ms, 9° tip angle, 144 slices 1 mm thick, 256×256 matrix over a 256×256 mm^2 field-of-view (FOV) and ×2 acceleration to guide the T_2^* imaging planes.

A coronal oblique volume-of-interest (VOI) was then image-guided onto the medial hippocampus, using the sagittal reformatted MP-RAGE MRI. It was placed with the slices' planes (approximately) perpendicular to the long axis of the structure, as seen on a sagittal guiding image and positioned to include as much of it as possible given the 17 slices (30.6 mm) width of the VOI, as shown in Figure 1. The VOI was then imaged with heavily T_2^*-weighted 2D gradient-echo sequence: *TR/TE*= 944/25 ms, 35° nutation, 238×238 mm^2 FOV, 1024×1024 matrix, ×1 acceleration. Acquiring 17 1.5 mm thick slices with 20% gap yielded 232×232×1500 μm^3=0.08 μL image voxel resolution, in 14 minutes. This voxel size suffices to visualize the smaller DGCL due to partial volume (in 1–2 voxels); and T_2^* field effects, as shown ex vivo in Figure 2 and in vivo in Figure 3 (Prudent et al., 2010).

All T_2^*-weighted images were read by three neuroradiologists blinded to the clinical diagnosis and to each other. Each scrolled through the 17 images and selected the one on which the DGCL looked best (left and right – not necessarily on the same slice). They then each rated the bilateral DGCL in every subject on a scale of 1 – 6 proposed by the senior radiologist to address the paucity of an existing method to grade the integrity of this structure at the subfield level, which is otherwise not resolved in routine clinical MRI at lower, 1.5 or 3 T magnetic fields. On this new scale a "1" indicates not discernible, "2" partially visible but faint, "3" <50% visible and appears light gray, "4" >50% visible and appears light gray, "5" entirely visible and appears light gray; and "6" easily visible, appearing dark gray or black. An example is given in Figure 4. A second blinded reading by the senior neuroradiologist was done to establish test-retest reliability.

2.3 Histological sample

The ex vivo hippocampus sample was fixed with formalin for two weeks, washed in water, and placed in 2% agarose (Sigma-Aldrich, St. Louis. MO) in phosphor-buffered saline and solidified in a 50 ml conical tube in order to fix its position. The same MRI acquisition protocol was run on that sample. The specimen was subsequently retrieved from the tube, serially sectioned in planes matching the coronal MRI as closely as possible (Figure 2) and processed for paraffin-embedded tissue block. The histopathology slides were then stained with Luxol-Fast Blue (LFB) combined with hemotoxylin-eosin (H&E) staining (Sheehan and Hrapchak, 1987), as shown in Figure 2c.

2.4 Statistical Analyses

Gender and age differences between patients and controls were assessed using a Fisher's exact test and an exact Mann-Whitney test, respectively. Given the qualitative nature of the data, a non-parametric Mann-Whitney test (two tailed) was used to compare patients to controls in terms of the mean right and left DGCL score. Since there does not exist a fully non-parametric way to compare the groups in terms of the left and right scores while adjusting for a numeric covariate such as age, no covariate analyses were performed. Gender and age were controlled for, however, in a logistic regression analysis with group (controls versus patients) as the binary outcome: gender and age were entered into the model at the first step, then right and left DGCL scores were entered using the backward stepping procedure. Based on a Receiver Operating Characteristic (ROC) curve analysis, the diagnostic utility of the left and right hemisphere scores was summarized in terms of the area under the ROC curve and in terms of sensitivity and specificity to predict diagnosis. Pearson and Spearman correlations were used to characterize the association between PANSS symptomatology and right and left DGCL score. The association between the left and right DGCL score was assessed using a Spearman rank correlation. Inter-reader agreement was assessed in terms of linear weighted kappa coefficients. Kappa (K) was interpreted as an indication of poor agreement when less than zero, as slight agreement when $0 \leq K \leq 0.2$, as fair agreement when $0.2 < K \leq 0.4$, as moderate agreement when $0.4 < K \leq 0.6$ and as substantial agreement when K>0.6 (Landis and Koch, 1977). MedCalc version 11.5.1.0 (Frank Schoonjans, Mariakerke, Belgium) was used for all computations.

3. RESULTS

3.1 Subjects

Nine patients (36%) and one control (6%) were excluded for excessive motion, leaving 16 patients (10 male, 6 female, 40.7±10.6 years old, 20±11 years mean illness duration) and 15 controls (8 male, 7 female, 35.6±9.4 years old) for analyses. Their demographic and clinical data are compiled in Table 1. There were no differences between the two groups in terms of gender (p=0.72) and age (p=0.22).

3.2 Validation of MRI with histology

To ascribe the thin gray layer on the in vivo MRI to the DGCL we compared the ex vivo hippocampus T_2^* weighted images (Figure 2a and b) with their approximately corresponding histopathology location, Figure 2c. Myelin, "My", highlighted by LFB staining on Figure 2c, appears as a broad hypo-intense (dark) layer on Figure 2b. The two layers ("4" and "5") on the inner side of the "My" layer, comprise the molecular and polymorphic layers. Between them, denoted by arrows, is the DGCL, appearing purple in Figure 2c. It is reasonable, therefore, to ascribe the thin gray strip (arrows) between "4" and "5" in Figure 2b, to the DGCL.

3.3 In vivo MRI

All hippocampal subfields, including the DGCL, were visible on the T_2^* images in patients and controls, as shown in Figures 3 and 4. The three neuroradiologists' gradings of the bilateral DGCL of every participant are compiled in Table 1. The average right DGCL ratings in patients and controls were 3.2±1.0 and 3.9±1.1 (p=0.07) and the average corresponding left DGCL ratings were 3.5±1.2 and 3.8±0.8 (p=0.4). The results from the logistic regression, which controlled for age and gender, showed that the (lower) right DGCL score was significantly associated with patient diagnosis (p=0.05), and that patients were 2.4× more likely to exhibit a lower right DGCL score than controls. There was a significant positive Spearman rank correlation between the right and left DGCL scores (r=0.72, $p < 0.001$). ROC analysis identified a right DGCL rating   2 as the optimal predictor of schizophrenia with 48% sensitivity (23/48 individual ratings, 3 radiologists ×16 patients) and 80% specificity (36/45 individual ratings). Inter-rater agreement was defined as "slight" with a maximal kappa of 0.13, which did not change when re-examined by the same blinded senior reader.

There were no statistically significant correlations between left or right DGCL ratings and any of the symptom domains assessed by the original PANSS scale and the pentagonal PANSS symptom factors. Finally, the average left or right DGCL ratings did not correlate with age of patients or controls, or with disease duration (all $r < 0.39$, $p > 0.05$).

4. DISCUSSION

Hippocampal DCGL, which is thought to underlie some of the neuropathological changes in schizophrenia, may be imaged with the high spatial resolution and tissue contrast at 7 Tesla MRI. The increases in overall sensitivity (Vaughan et al., 2001) and T_2^* contrast (Novak et al., 2005), combined with shimming and close-fitting 24 element coil array, offer spatial resolution and contrast superior to clinical 1.5 and 3.0 Tesla imagers (Theysohn et al., 2009; Thomas et al., 2008). The ~100 micron DGCL, however, is unique among the hippocampal subfields in that its thickness is below the current MRI pixel resolution even at 7 Tesla. The ability to visualize it, therefore, is due to several other factors including partial volume (in 1–2 voxels) and T_2^* field effects (Boretius et al., 2009; Li et al., 2006; Prudent et al., 2010). These preclude accurate volumetric analysis of the DGCL even with the recently developed manual and automated hippocampal segmentation software tools (Mueller et al., 2007; Van Leemput et al., 2008; Van Leemput et al., 2009; Yushkevich, 2010), and thus necessitated a qualitative assessment.

Patients had a statistical trend for decrease in DGCL contrast in the right hippocampus and this decrease was predictive of schizophrenia diagnosis. The nature of the lateral asymmetry is unclear since left/right DGCL histopathology differences have not been reported and volumetric studies of the dentate gyrus are lacking. Entire hippocampus structural studies may not be as relevant and have conflicting data on lateralization (Adriano et al., 2012; Harrison, 2004; Shenton et al., 2001). Nevertheless, we note that disease duration (~20 years in our cohort) has been linked to lower right hippocampal volume (Penttila et al., 2010; Velakoulis et al., 1999; Velakoulis et al., 2002), and that the right hippocampus is slightly larger in both patients and controls (Adriano et al., 2012; Harrison, 2004), potentially making contrast easier to discern.

The main reason for the hypointense appearance of the DGCL on the GRE images is a faster rate of T_2^* relaxation, which leads to signal intensity loss. T_2^* relaxation is a combination of "true" T_2 relaxation and relaxation caused by magnetic field inhomogeneities (Chavhan et al., 2009). As a result, a variety of effects may underlie the fact that lower contrast was linked to schizophrenia diagnosis. One explanation concerns the quantity of free water.

Neuronal density, organization and architecture influence the amount of intracellular and extracellular water, which give rise to the MR signal. An increase in water content as a result of any of these processes will translate in a more hyperintense signal, i.e. loss of contrast in the DGCL. Of note, increased water content also prolongs the T_1 relaxation time, which could also contribute to increased hyperintensity. Magnetic field inhomogeneities from susceptibility differences among tissues also cause faster T_2* relaxation. For example, loss of hypointense contrast in schizophrenia DGCL may be explained by lower iron concentrations or decreased mircovascularity (deoxyhemoglobin), although histopathological reports of either are lacking. Unfortunately, using only GRE imaging it is not possible to disentangle these effects and implicate the reason for the hypointense DGCL and consequently, its contrast changes. Because spin-echo sequences abolish magnetic field susceptibility effects, if the DGCL can be distinguished using such technique, the possible scenarios would be constrained, but not to the extent of pinpointing a single source of contrast.

An increase of intra and/or extracellular water is the most likely of the above scenarios given the current neuropathology evidence of altered neuronal morphology, organization and synaptic parameters (Harrison, 2004), properties also controlled by many schizophrenia susceptibility genes expressed in the DGCL (Harrison and Weinberger, 2005). Neurodegeneration is not observed in schizophrenia hippocampi (Harrison, 2004), but decreases in cell density within the DGCL may occur in a scenario of decreased neurogenesis. Despite some evidence (Reif et al., 2006), however, it is unclear if this occurs in patients with schizophrenia (DeCarolis and Eisch, 2010) and if so, whether it is independent from stress, alcohol, smoking and drug abuse, all of which have been associated with decreased hippocampal neurogenesis (Cho and Kim, 2010; Warner-Schmidt and Duman, 2006). Further confounding this interpretation is data suggesting an opposite (pro-neurogenesis) effect of anti-psychotic medications (Cho and Kim, 2010; DeCarolis and Eisch, 2010). Unfortunately, the small sample size and the large number of potential confounds (phenotypic as well as genotypic, e.g. DISC-1 mutation status) undermine the utility of correlation testing in regards to elucidating a cause for the radiological phenomenon. Indeed, it is known that different subgroups of patients show different degrees and extent of structural deficits, and some effects may not be evident in all patients (Nenadic et al., 2012). Since schizophrenia is a heterogeneous illness it is unlikely that DGCL disruptions or any other single marker would represent all patients. Hence, examining homogenous patient groups may increase the sensitivity and specificity to levels that may aid in diagnosis for individual patients and in development and monitoring of new therapies.

While this is the first 7 Tesla MRI study in schizophrenia, ultra high field imaging has the potential to address a number of unanswered questions about the in vivo characteristics of the disease. The advantages of increased resolution and signal-to-noise ratio can be exploited with different techniques, depending on their capabilities and the region of interest. Due to the increased susceptibility effects at higher field, T_2*-weighted images experience a large gain in tissue contrast. Among the schizophrenia-relevant regions of interest, applications of T_2*-weighted imaging at 7 Tesla have shown differences in contrast (i.e. increased resolution) within the substantia nigra and the red nucleus in the midbrain (Eapen et al., 2011) and within the cerebellar cortex (Marques et al., 2010). In addition to increased contrast within gray matter, T_2*-weighted imaging has shown large heterogeneity within white matter (Li et al., 2006), providing a tool to test hypotheses involving specific tracts. While less sensitive to intra-tissue differences, T_1- and T_2-weighted imaging is traditionally valued for its inter-tissue (gray/white matter) contrast. As a result, both techniques have been used at high field for segmentation of hippocampal subfields (Mueller et al., 2007; Wisse et al., 2012), which may be particularly useful in schizophrenia given the

evidence for regional specificity in hippocampal volume deficits (Narr et al., 2004; Schobel et al., 2009a).

This study is also subject to several limitations. First, it is insufficiently powered to analyze effects of disease phenotype, or to adequately account for confounding conditions, e.g. smoking, known to affect the hippocampus. Second, it was not possible to test the sensitivity and specificity metrics found in these subjects on an additional group of patients and controls, nor was it practical to split the current groups into "training" and "testing" sets for post hoc validation. Third, we could not control for possible medication effects, a limitation that given ethical considerations, is unavoidable. Fourth, the exquisite resolution at 7 Tesla is susceptible to miniscule motion, and as a result, involuntary patient movement (likely due to the extrapyramidal side effects of the antipsychotic medication) led to the exclusion of more than 30% of patients. A quantitative approach to recognizing motion-corrupted data, however, might be helpful in reducing exclusion bias in future studies. Finally, although three radiologists read the images, the novelty of 7 Tesla hippocampal MRI limited the usefulness of their experience, as reflected by the small inter- and intra-rater Kappa. More experience in hippocampal subfield imaging may refine the rating scale to improve sensitivity, specificity and concordance.

Acknowledgments

References

Adriano F, Caltagirone C, Spalletta G. Hippocampal volume reduction in first-episode and chronic schizophrenia: a review and meta-analysis. Neuroscientist. 2012; 18(2):180–200. [PubMed: 21531988]

Altar CA, Jurata LW, Charles V, Lemire A, Liu P, Bukhman Y, Young TA, Bullard J, Yokoe H, Webster MJ, Knable MB, Brockman JA. Deficient hippocampal neuron expression of proteasome, ubiquitin, and mitochondrial genes in multiple schizophrenia cohorts. Biol Psychiatry. 2005; 58(2): 85–96. [PubMed: 16038679]

Bast T. The hippocampal learning-behavior translation and the functional significance of hippocampal dysfunction in schizophrenia. Curr Opin Neurobiol. 2011; 21(3):492–501. [PubMed: 21330132]

Benetti S, Mechelli A, Picchioni M, Broome M, Williams S, McGuire P. Functional integration between the posterior hippocampus and prefrontal cortex is impaired in both first episode schizophrenia and the at risk mental state. Brain. 2009; 132(Pt 9):2426–36. [PubMed: 19420091]

Boretius S, Kasper L, Tammer R, Michaelis T, Frahm J. MRI of cellular layers in mouse brain in vivo. Neuroimage. 2009; 47(4):1252–60. [PubMed: 19520174]

Chavhan GB, Babyn PS, Thomas B, Shroff MM, Haacke EM. Principles, techniques, and applications of T2*-based MR imaging and its special applications. Radiographics. 2009; 29(5):1433–49. [PubMed: 19755604]

Cho KO, Kim SY. Effects of brain insults and pharmacological manipulations on the adult hippocampal neurogenesis. Arch Pharm Res. 2010; 33(10):1475–88. [PubMed: 21052928]

DeCarolis NA, Eisch AJ. Hippocampal neurogenesis as a target for the treatment of mental illness: a critical evaluation. Neuropharmacology. 2010; 58(6):884–93. [PubMed: 20060007]

Eapen M, Zald DH, Gatenby JC, Ding Z, Gore JC. Using high-resolution MR imaging at 7T to evaluate the anatomy of the midbrain dopaminergic system. AJNR Am J Neuroradiol. 2011; 32(4): 688–94. [PubMed: 21183619]

Harrison PJ. The hippocampus in schizophrenia: a review of the neuropathological evidence and its pathophysiological implications. Psychopharmacology (Berl). 2004; 174(1):151–62. [PubMed: 15205886]

Harrison PJ, Weinberger DR. Schizophrenia genes, gene expression, and neuropathology: on the matter of their convergence. Mol Psychiatry. 2005; 10(1):40–68. image 5. [PubMed: 15263907]

Kay SR, Fiszbein A, Opler LA. The positive and negative syndrome scale (PANSS) for schizophrenia. Schizophr Bull. 1987; 13(2):261–76. [PubMed: 3616518]

Kay, SR.; Fiszbein, A.; Opler, LA. Positive and Negative Syndrome Scale (PANSS) Manual. Toronto: 1992.

Kay SR, Opler LA, Lindenmayer JP. The Positive and Negative Syndrome Scale (PANSS): rationale and standardisation. Br J Psychiatry. 1989; (Suppl 7):59–67.

Landis JR, Koch GG. The measurement of observer agreement for categorical data. Biometrics. 1977; 33(1):159–74. [PubMed: 843571]

Larson MK, Walker EF, Compton MT. Early signs, diagnosis and therapeutics of the prodromal phase of schizophrenia and related psychotic disorders. Expert Rev Neurother. 2010; 10(8):1347–59. [PubMed: 20662758]

Lauer M, Beckmann H, Senitz D. Increased frequency of dentate granule cells with basal dendrites in the hippocampal formation of schizophrenics. Psychiatry Res. 2003; 122(2):89–97. [PubMed: 12714173]

Law AJ, Shannon Weickert C, Hyde TM, Kleinman JE, Harrison PJ. Neuregulin-1 (NRG-1) mRNA and protein in the adult human brain. Neuroscience. 2004; 127(1):125–36. [PubMed: 15219675]

Li TQ, van Gelderen P, Merkle H, Talagala L, Koretsky AP, Duyn J. Extensive heterogeneity in white matter intensity in high-resolution T2*-weighted MRI of the human brain at 7.0 T. Neuroimage. 2006; 32(3):1032–40. [PubMed: 16854600]

Marques JP, van der Zwaag W, Granziera C, Krueger G, Gruetter R. Cerebellar cortical layers: in vivo visualization with structural high-field-strength MR imaging. Radiology. 2010; 254(3):942–8. [PubMed: 20177104]

Meyer KD, Morris JA. Disc1 regulates granule cell migration in the developing hippocampus. Hum Mol Genet. 2009; 18(17):3286–97. [PubMed: 19502360]

Ming GL, Song H. Adult neurogenesis in the mammalian brain: significant answers and significant questions. Neuron. 2011; 70(4):687–702. [PubMed: 21609825]

Mueller SG, Stables L, Du AT, Schuff N, Truran D, Cashdollar N, Weiner MW. Measurement of hippocampal subfields and age-related changes with high resolution MRI at 4T. Neurobiol Aging. 2007; 28(5):719–26. [PubMed: 16713659]

Mueser KT, Penn DL. Meta-analysis examining the effects of social skills training on schizophrenia. Psychol Med. 2004; 34(7):1365–7. [PubMed: 15697062]

Narr KL, Thompson PM, Szeszko P, Robinson D, Jang S, Woods RP, Kim S, Hayashi KM, Asunction D, Toga AW, Bilder RM. Regional specificity of hippocampal volume reductions in first-episode schizophrenia. Neuroimage. 2004; 21(4):1563–75. [PubMed: 15050580]

Nenadic I, Gaser C, Sauer H. Heterogeneity of brain structural variation and the structural imaging endophenotypes in schizophrenia. Neuropsychobiology. 2012; 66(1):44–9. [PubMed: 22797276]

Novak V, Abduljalil AM, Novak P, Robitaille PM. High-resolution ultrahigh-field MRI of stroke. Magn Reson Imaging. 2005; 23(4):539–48. [PubMed: 15919599]

Nurnberger JI Jr, Blehar MC, Kaufmann CA, York-Cooler C, Simpson SG, Harkavy-Friedman J, Severe JB, Malaspina D, Reich T. Diagnostic interview for genetic studies. Rationale, unique features, and training. NIMH Genetics Initiative. Arch Gen Psychiatry. 1994; 51(11):849–59. discussion 863–4. [PubMed: 7944874]

Penttila M, Jaaskelainen E, Haapea M, Tanskanen P, Veijola J, Ridler K, Murray GK, Barnes A, Jones PB, Isohanni M, Koponen H, Miettunen J. Association between duration of untreated psychosis and brain morphology in schizophrenia within the Northern Finland 1966 Birth Cohort. Schizophrenia research. 2010; 123(2–3):145–52. [PubMed: 20832996]

Prudent V, Kumar A, Liu S, Wiggins G, Malaspina D, Gonen O. Human hippocampal subfields in young adults at 7.0 T: feasibility of imaging. Radiology. 2010; 254(3):900–6. [PubMed: 20123900]

Reif A, Fritzen S, Finger M, Strobel A, Lauer M, Schmitt A, Lesch KP. Neural stem cell proliferation is decreased in schizophrenia, but not in depression. Mol Psychiatry. 2006; 11(5):514–22. [PubMed: 16415915]

Rioux L, Arnold SE. The expression of retinoic acid receptor alpha is increased in the granule cells of the dentate gyrus in schizophrenia. Psychiatry Res. 2005; 133(1):13–21. [PubMed: 15698673]

Schobel SA, Kelly MA, Corcoran CM, Van Heertum K, Seckinger R, Goetz R, Harkavy-Friedman J, Malaspina D. Anterior hippocampal and orbitofrontal cortical structural brain abnormalities in association with cognitive deficits in schizophrenia. Schizophr Res. 2009a; 114(1–3):110–8. [PubMed: 19683896]

Schobel SA, Lewandowski NM, Corcoran CM, Moore H, Brown T, Malaspina D, Small SA. Differential targeting of the CA1 subfield of the hippocampal formation by schizophrenia and related psychotic disorders. Arch Gen Psychiatry. 2009b; 66(9):938–46. [PubMed: 19736350]

Sheehan, DC.; Hrapchak, B. Theory and practice of Histotechnology. Ohio: Battelle Press; 1987.

Shenton ME, Dickey CC, Frumin M, McCarley RW. A review of MRI findings in schizophrenia. Schizophr Res. 2001; 49(1–2):1–52. [PubMed: 11343862]

Small SA, Schobel SA, Buxton RB, Witter MP, Barnes CA. A pathophysiological framework of hippocampal dysfunction in ageing and disease. Nat Rev Neurosci. 2011; 12(10):585–601. [PubMed: 21897434]

Tamminga CA, Stan AD, Wagner AD. The hippocampal formation in schizophrenia. Am J Psychiatry. 2010; 167(10):1178–93. [PubMed: 20810471]

Theysohn JM, Kraff O, Maderwald S, Schlamann MU, de Greiff A, Forsting M, Ladd SC, Ladd ME, Gizewski ER. The human hippocampus at 7 T--in vivo MRI. Hippocampus. 2009; 19(1):1–7. [PubMed: 18727048]

Thomas BP, Welch EB, Niederhauser BD, Whetsell WO Jr, Anderson AW, Gore JC, Avison MJ, Creasy JL. High-resolution 7T MRI of the human hippocampus in vivo. J Magn Reson Imaging. 2008; 28(5):1266–72. [PubMed: 18972336]

Van Leemput K, Bakkour A, Benner T, Wiggins G, Wald LL, Augustinack J, Dickerson BC, Golland P, Fischl B. Model-based segmentation of hippocampal subfields in ultra-high resolution in vivo MRI. Med Image Comput Comput Assist Interv Int Conf Med Image Comput Comput Assist Interv. 2008; 11(Pt 1):235–43.

Van Leemput K, Bakkour A, Benner T, Wiggins G, Wald LL, Augustinack J, Dickerson BC, Golland P, Fischl B. Automated segmentation of hippocampal subfields from ultra-high resolution in vivo MRI. Hippocampus. 2009

Vaughan JT, Garwood M, Collins CM, Liu W, DelaBarre L, Adriany G, Andersen P, Merkle H, Goebel R, Smith MB, Ugurbil K. 7T vs. 4T: RF power, homogeneity, and signal-to-noise comparison in head images. Magn Reson Med. 2001; 46(1):24–30. [PubMed: 11443707]

Velakoulis D, Pantelis C, McGorry PD, Dudgeon P, Brewer W, Cook M, Desmond P, Bridle N, Tierney P, Murrie V, Singh B, Copolov D. Hippocampal volume in first-episode psychoses and chronic schizophrenia: a high-resolution magnetic resonance imaging study. Archives of general psychiatry. 1999; 56(2):133–41. [PubMed: 10025437]

Velakoulis D, Wood SJ, Smith DJ, Soulsby B, Brewer W, Leeton L, Desmond P, Suckling J, Bullmore ET, McGuire PK, Pantelis C. Increased duration of illness is associated with reduced volume in right medial temporal/anterior cingulate grey matter in patients with chronic schizophrenia. Schizophrenia research. 2002; 57(1):43–9. [PubMed: 12165375]

Warner-Schmidt JL, Duman RS. Hippocampal neurogenesis: opposing effects of stress and antidepressant treatment. Hippocampus. 2006; 16(3):239–49. [PubMed: 16425236]

Weickert CS, Rothmond DA, Hyde TM, Kleinman JE, Straub RE. Reduced DTNBP1 (dysbindin-1) mRNA in the hippocampal formation of schizophrenia patients. Schizophr Res. 2008; 98(1–3): 105–10. [PubMed: 17961984]

White L, Harvey PD, Opler L, Lindenmayer JP. Empirical assessment of the factorial structure of clinical symptoms in schizophrenia. A multisite, multimodel evaluation of the factorial structure of the Positive and Negative Syndrome Scale. The PANSS Study Group. Psychopathology. 1997; 30(5):263–74. [PubMed: 9353855]

Wisse LE, Gerritsen L, Zwanenburg JJ, Kuijf HJ, Luijten PR, Biessels GJ, Geerlings MI. Subfields of the hippocampal formation at 7 T MRI: in vivo volumetric assessment. Neuroimage. 2012; 61(4): 1043–9. [PubMed: 22440643]

Yushkevich PA, Wang H, Pluta J, Das SR, Craige C, Avants BB, Weiner MW, Mueller S. Nearly automatic segmentation of hippocampal subfields in in vivo focal T2-weighted MRI. Neuroimage. 2010; 53(4):1208–24. [PubMed: 20600984]
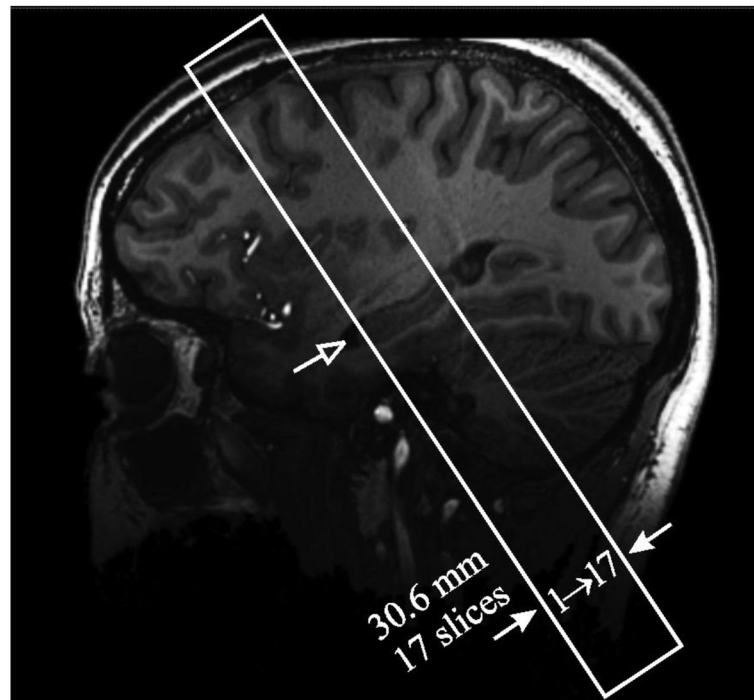
Figure 1.
Sagittal T_1-weighted MP-RAGE slice of a 21 year old female control (#17 in Table 1) showing the oblique VOI (solid frame) placement over the hippocampus mid-body region (open arrow).
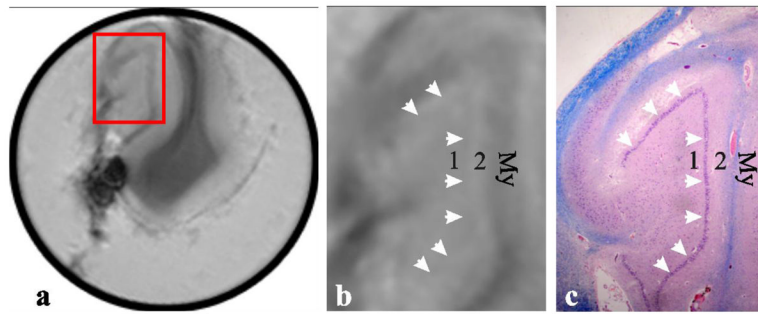
Figure 2.

<u>Left, (**a**)</u>: Coronal heavily T_2^*- weighted MRI of a post-mortem ex-vivo hippocampus from a 68 year old woman who died of pneumonia. Red frame indicates the region expanded on (**b**) and (**c**).

<u>Center, (**b**)</u>: Magnified view of area within the red frame in (**a**)

<u>Right, (**c**)</u>: Low power (×2) view of the corresponding histology section stained with LFB combined with H&E.

The dentate gyrus comprises 3 layers: "1," a polymorphic layer containing nerve fibers ("mossy fibers") and cell bodies of interneurons; "2" a molecular layer containing dendrites of the granule cells. The third and middle layer, the dentate granule cell layer (DGCL), contains the round, neuronal cell bodies of dentate granule cells and is indicated by white arrows on (**b**) and (**c**). "My" indicates myelinated fibers. Note the correspondence between anatomical detail, especially the well defined DGCL on the histopathology slice, (**c**), and the faint albeit distinct structure on the T_2^*-weighted MRI, (**a**) and (**b**).
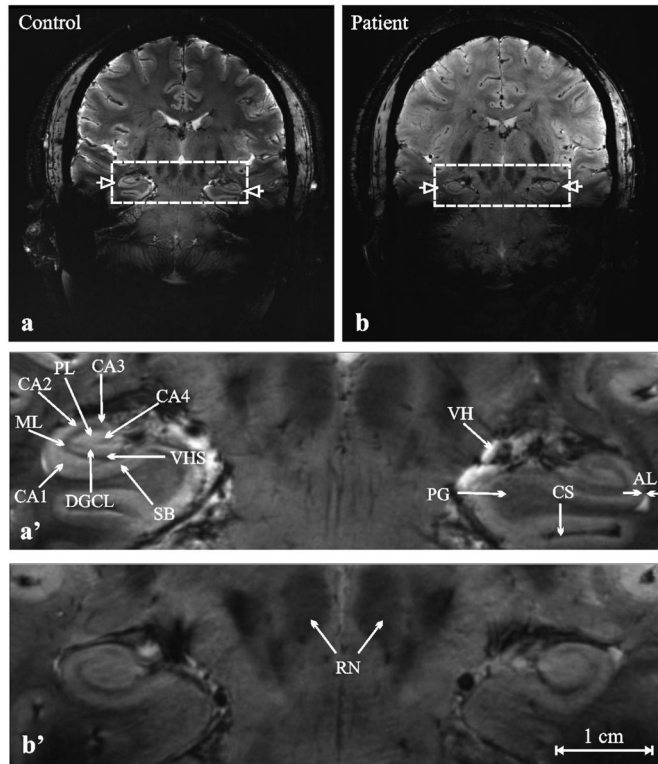
Figure 3.
<u>Top, **a**, **b**</u>: Coronal heavily T_2^*- weighted MRI of (**a**) 43 year old male control (#28 in Table 1) and (**b**) 29 year old female schizophrenia patient (#3 in Table 1). Left and right hippocampi are indicated with open arrows.
<u>Bottom, **a**′, **b**′</u>: Magnification of the area in the dashed frames of (**a**) and (**b**).
Arrows indicate the following structures: AL- alveus, CA1…4 cornu ammonis, CS- collateral sulcus, dentate granule cell layer (DGCL), ML- molecular layer of the dentate gyrus, PL- polymorphic layer of the dentate gyrus, PG- parahippocampal gyrus, RN- red nuclei, SB- subiculum, VH- ventricular horn, VHS- vestigial hippocampal sulcus. Note the subfield anatomic detail and exquisite contrast achievable in 14 minutes at 7 Tesla.
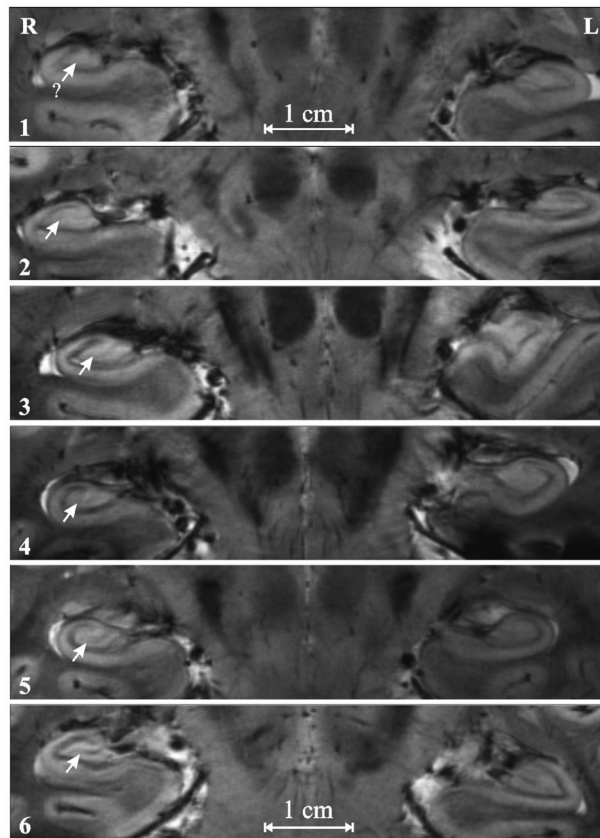
Figure 4.
Examples of the 1 – 6 DGCL (arrows) integrity rating scale used: From top to bottom: **1:** Not discernible; **2:** partially visible but faint; **3:** <50% visible and appear light gray; **4:** 50% visible and light gray in appearance; **5:** Entirely visible and appears light gray; **6:** Entire DGCL is easily visualized and appears dark gray or black.

Table 1

Demographics and mean (of the three readers) hippocampal DGCL ratings for all patients (1–16) and controls (17–31) on a scale of 1 – 6.

	[a] Age/gender	[a] Disease duration	Medication	Mean DGCL rating	
				Right	Left
1	23/M	3	Risperidone	2.3	2.7
2	26/M	8	Ziprasidone	2.3	1.7
3	29/F	8	Aripiprazole, Bupropion, Fluphenazine	4.3	4
4	29/M	9	Clomipramine, Clonazepam, Risperidone,	4.0	5.7
5	29/F	9	Aripiprazole	3.3	4.3
6	35/M	6	Risperidone	2.3	3.0
7	42/F	23	Bupropion, Eszopiclone, Ziprasidone	2.0	2.3
8	43/M	18	Halperidol, Quetiapine	4.0	3.7
9	44/M	26	Clozapine, Valproic Acid	3.0	4.7
10	44/F	27	Quetiapine	2.3	2.3
11	49/F	31	Aripiprazole	4.3	5.0
12	51/M	31	Risperidone	1.7	2.3
13	51/F	35	-	4.0	4.3
14	52/M	32	Citalopram	3.0	2.7
15	52/M	22	Aripiprazole, Paroxetine, Trazadone, Valproic Acid	5.0	4.3
16	53/M	31	Clozapine, Gabapentin, Venlafaxine	2.7	3.3
17	21/F	-	-	3.0	3.7
18	23/M	-	-	4.0	3.3
19	27/F	-	-	3.7	3.3
20	29/F	-	-	2.7	3.3
21	31/F	-	-	5.3	4.3
22	31/M	-	-	3.0	2.7
23	34/F	-	-	5.3	4.7
24	36/M	-	-	2.3	4.0
25	37/F	-	-	3.7	3.7
26	37/M	-	-	3.7	4.0

	^a Age/gender	^a Disease duration	Medication	Mean DGCL rating	
				Right	**Left**
27	38/M	-	-	3.3	3.0
28	43/M	-	-	5.7	5.7
29	46/M	-	-	4.7	4.3
30	47/M	-	-	5.0	3.3
31	55/F	-	-	3.3	4.3

^aYears.